Derivation of a neural field model from a network of theta neurons

Carlo R. Laing*
Institute of Natural and Mathematical Sciences, Massey University,
Private Bag 102-904 NSMC, Auckland, New Zealand.
phone: +64-9-414 0800 extn. 41038 fax: +64-9-4418136
(Dated: July 21, 2014)

Neural field models are used to study macroscopic spatio-temporal patterns in the cortex. Their derivation from networks of model neurons normally involves a number of assumptions, which may not be correct. Here we present an exact derivation of a neural field model from an infinite network of theta neurons, the canonical form of a Type I neuron. We demonstrate the existence of a "bump" solution in both a discrete network of neurons and in the corresponding neural field model.

PACS numbers: 05.45.Xt, 87.19.ll
Keywords: neural field, theta neuron, Ott/Antonsen

Large-scale coherent activity in the brain is associated with a variety of behaviour such as an epileptic seizure or remembering something in short term memory [1, 2]. A number of "neural field" models have been proposed to explain such activity, and these models have been studied intensively over a number of decades [3–10]. While such models have been successful in helping to understand phenomena as diverse as visual hallucinations [5], binocular rivalry [6], and the head direction system [11], a significant issue with neural field models is their relationship to — and derivation from — networks of individual neurons. Neural field models normally take the form of nonlocal partial differential equations in space and time for a variable that is interpreted as "synaptic drive" or the average voltage difference between the inside of a neuron and the outside. In deriving such models from networks of neurons a number of assumptions are made, such as a separation of timescales between neuron and synaptic dynamics [3, 5]. These assumptions may not necessarily hold.

In this paper we derive exactly a neural field model from an infinite network of "theta neurons". The theta neuron is the normal form of a Type I neuron, for which the onset of firing occurs through a saddle-node-on-a-circle bifurcation as the input current is increased [12]. While the derivation is only exact for an infinite network, we find that it predicts well the behaviour of a large finite network. The derivation requires the form of communication between two neurons to be of a particular form, but the coupling architecture can be arbitrary. Our work builds on previous results for a network with no spatial structure [13, 14].

The discrete model we consider consists of a network of N theta neurons on a one-dimensional domain of length L. The state of neuron j at time t is $\theta_j(t) \in [0, 2\pi]$ and the dynamics of the network is

$$\frac{d\theta_j}{dt} = 1-\cos\theta_j+(1+\cos\theta_j)(\eta_j+kI_j); \quad j = 1,\dots N \quad (1)$$

where the input to neuron j from other neurons in the network is

$$I_j = \frac{L}{N}\sum_{i=1}^{N} K_{ji}P_n(\theta_i). \quad (2)$$

The parameter k is an overall coupling strength, and $P_n(\theta) = a_n(1-\cos\theta)^n$, $n \in \mathbb{N}^+$, is a "pulse-like" function, where a_n is chosen so that $\int_0^{2\pi} P_n(\theta)d\theta = 2\pi$. P_n has a maximum at $\theta = \pi$, and increasing n increases the "sharpness" of this function. In the limit as $n \to \infty$, i.e. for impulsive synapses, we have $P_\infty(\theta) = 2\pi\delta(\theta-\pi)$. The coupling from neuron i to neuron j depends on only the difference $|j-i|$ (i.e. the distance between neurons) and is given by

$$K_{ji} = K(|j-i|\Delta x) \quad (3)$$

where $\Delta x = L/N$ and the function K will be specified below. The neurons are assumed to be heterogeneous, and we model this by randomly and independently choosing the η_j from the Lorentzian distribution with mean η_0 and width Δ:

$$g(\eta) = \frac{\Delta/\pi}{(\eta-\eta_0)^2+\Delta^2} \quad (4)$$

The value of η_j governs neuron j's behaviour in the absence of input: if $\eta_j < 0$ the neuron is excitable, whereas if $\eta_j > 0$, the neuron fires periodically. Thus $\eta_j = 0$ is the threshold for firing.

We consider the "Mexican-hat" coupling function $K(x) = 0.1 + 0.3\cos x$ on the spatial domain $[0, 2\pi]$, with periodic boundary conditions. This type of coupling function means that nearby neurons excite one another but inhibit more distant ones, and is commonly used in modelling studies [3]. A periodic domain is appropriate if x represents an angular variable such as head direction.

A typical example of the dynamics of (1)-(2) with $N = 600$ is shown in Fig. 1. This state is a "bump" state, as observed in a number of other simulations of discrete networks of neurons [15, 16]. Neurons in part of the domain are quiescent, while others are firing approximately periodically. The firing frequency is a maximum

*Electronic address: c.r.laing@massey.ac.nz

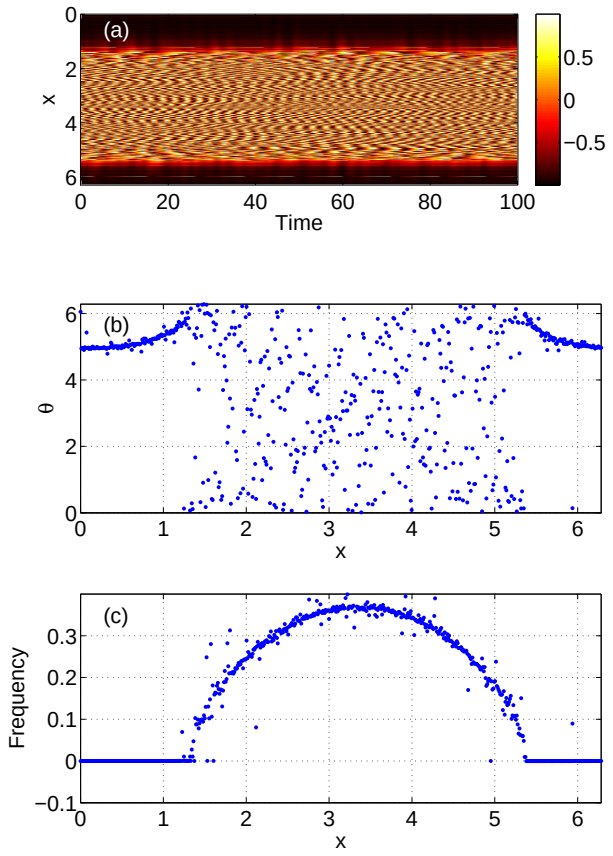

Figure 1: (Color online) A simulation of (1)-(4) with coupling function $K(x) = 0.1 + 0.3\cos x$. (a): $\sin\theta$, colour-coded. (b): snapshot of the network at $t = 100$. (c): average firing frequency over $0 \le t \le 100$. Parameters: $L = 2\pi, k = 2, N = 600, n = 2, \eta_0 = -0.4, \Delta = 0.02$.

in the centre of the bump, falling continuously to zero at its edges. Such states are thought to play a role in short term memory [17], since for these parameter values the network is bistable; the "all off" state, where most neurons are quiescent, is also stable (not shown). The position of the bump in the network is determined by the transient stimulus that moved the network into the bump state (the transient contains the information to be "remembered"), and this information can be retrieved at a later time by determining the position of the fastest firing neuron. Similar bump states exist in this network at these parameter values for N as small as 40, although finite size effects, in the form of "wandering" of the bump, do become more prominent as N decreases.

We now take the continuum limit, $N \to \infty$, of the discrete network and exactly derive the corresponding neural field model. In this limit, the system is described by the probability density function $F(x, \eta, \theta, t)$, such that $F(x, \eta, \theta, t)dx\ d\eta\ d\theta$ is the probability that a neuron in $(x, x + dx)$ has a value of η in $(\eta, \eta + d\eta)$ and phase in $(\theta, \theta + d\theta)$ at time t [18, 19]. This function satisfies the continuity equation

$$\frac{\partial F}{\partial t} + \frac{\partial}{\partial \theta}(Fv) = 0 \tag{5}$$

where v is the continuum limit of the right hand side (RHS) of (1):

$$v(x, \theta, \eta, t) \equiv 1 - \cos\theta + (1 + \cos\theta)[\eta + kI(x, t)] \tag{6}$$

where

$$I(x,t) = \int_0^L K(x-y) \int_{-\infty}^{\infty} \int_0^{2\pi} F(y, \eta, \theta, t) a_n (1-\cos\theta)^n d\theta d\eta dy \tag{7}$$

We also introduce the complex, space-dependent, order parameter (the expected value of $e^{i\theta}$)

$$z(x,t) = \int_{-\infty}^{\infty} \int_0^{2\pi} F(x, \eta, \theta, t) e^{i\theta} d\theta\ d\eta \tag{8}$$

and below we derive a closed equation for the evolution of z; this is the neural field model. To simplify (5)-(7) we use the Ott/Antonsen ansatz [20, 21], i.e. we write

$$F(x, \eta, \theta, t) = \frac{g(\eta)}{2\pi} \left\{ 1 + \sum_{q=1}^{\infty} [\alpha(x, \eta, t)]^q\, e^{iq\theta} + c.c. \right\} \tag{9}$$

where "$c.c.$" is the complex conjugate of the preceding term and α is a complex-valued function. Substituting (9) into (8) we obtain

$$z(x,t) = \int_{-\infty}^{\infty} g(\eta) \bar{\alpha}(x, \eta, t) d\eta \tag{10}$$

and using standard properties of the Lorentzian to perform the integration over η [13, 18] we obtain $z(x,t) = \bar{\alpha}(x, \eta_0 - i\Delta, t)$, where an overbar indicates complex conjugation. Now So et al. [13] showed that

$$(1 - \cos\theta)^n = \sum_{k=0}^{n} \sum_{m=0}^{k} Q_{km} e^{i(k-2m)\theta} \tag{11}$$

where

$$Q_{km} = \frac{n!(-1)^k}{2^k (n-k)! m! (k-m)!} \tag{12}$$

and thus using (9) we obtain

$$\int_0^{2\pi} F(y, \eta, \theta, t) a_n (1 - \cos\theta)^n d\theta$$
$$= a_n g(\eta) \left(C_0 + \sum_{q=1}^{n} C_q \left\{ [\alpha(y, \eta, t)]^q + [\bar{\alpha}(y, \eta, t)]^q \right\} \right) \tag{13}$$

where

$$C_q = \sum_{k=0}^{n} \sum_{m=0}^{k} \delta_{k-2m,q} Q_{km} \tag{14}$$

where $\delta_{i,j}$ is the Kronecker delta. Using this result and the properties of the Lorentzian $g(\eta)$ one can show that

$$\int_{-\infty}^{\infty} g(\eta)\left(C_0+\sum_{q=1}^{n} C_q\left\{[\alpha(y,\eta,t)]^q+[\bar{\alpha}(y,\eta,t)]^q\right\}\right)d\eta$$
$$=C_0+\sum_{q=1}^{n} C_q\left\{[z(y,t)]^q+[\bar{z}(y,t)]^q\right\} \tag{15}$$

Thus

$$I(x,t)=\int_0^L K(x-y)H(z(y,t);n)dy \tag{16}$$

where

$$H(z;n)=a_n\left[C_0+\sum_{q=1}^{n} C_q\left(z^q+\bar{z}^q\right)\right] \tag{17}$$

(It can be shown that for impulsive coupling, $H(z;\infty)=(1-|z|^2)/(1+z+\bar{z}+|z|^2)$.)

Now from the form of v we know that α satisfies [22]

$$\frac{\partial\alpha}{\partial t}=-i\left[\frac{\eta+kI-1}{2}+(1+\eta+kI)\alpha+\left(\frac{\eta+kI-1}{2}\right)\alpha^2\right] \tag{18}$$

and evaluating this at $\eta=\eta_0-i\Delta$ and simplifying we obtain

$$\frac{\partial z}{\partial t}=\frac{(i\eta_0-\Delta)(1+z)^2-i(1-z)^2}{2}+k\frac{i(1+z)^2}{2}I \tag{19}$$

This is our neural field equation, a nonlocal partial differential equation. The first term on the RHS of (19) governs the local dynamics in the absence of input from the rest of the network, and the second term describes the contributions of the rest of the network to the dynamics at position x through the integral (16).

Equation (19) is not in the usual form of a neural field equation, since it is not immediately clear what the physical interpretation of z is, and quantities such as the firing rate of neurons (that normally appear in neural field models) do not appear explicitly in (19). For the physical interpretation, write z in polar form as $z(x,t)=r(x,t)e^{i\psi(x,t)}$, then marginalise (9) over η to obtain the probability density function

$$p(\theta,x,t)=\frac{1-r^2(x,t)}{2\pi\{1-2r(x,t)\cos[\theta-\psi(x,t)]+r^2(x,t)\}} \tag{20}$$

At fixed x and t this is a unimodal function of θ with a maximum at $\theta=\psi$, and whose sharpness is governed by the value of r [18], i.e. the magnitude and phase of z describe the distribution of phases, θ. As for the firing rate, in the discrete network the total input to neuron j is η_j+kI_j and its frequency is $\sqrt{\eta_j+kI_j}/\pi$ [12]. Thus in the continuum limit the frequency of neurons at position x and time t is

$$f(x,t)=\frac{1}{\pi}\int_{-kI(x,t)}^{\infty} g(\eta)\sqrt{\eta+kI(x,t)}d\eta \tag{21}$$
$$=\sqrt{\frac{\eta_0+kI(x,t)+\sqrt{[\eta_0+kI(x,t)]^2+\Delta^2}}{2\pi^2}} \tag{22}$$

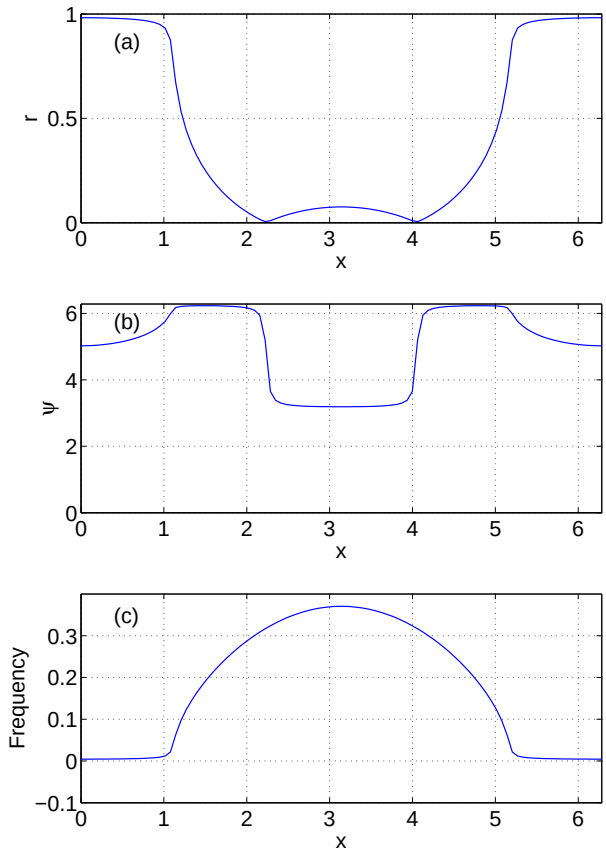

Figure 2: Steady state of (19). Compare with Fig. 1. (a): magnitude of z. (b): argument of z. (c): Frequency, as given by (22). Parameters: $L=2\pi, k=2, n=2, \eta_0=-0.4, \Delta=0.02$.

A steady state of (19) is shown in Fig. 2, together with the frequency profile [1]. Note that the system is invariant with respect to translations in x, so this is one of a continuous family of solutions, each related to one another by a shift in x. We see that away from the centre of the domain, the magnitude of z is close to 1, indicating near synchrony. The neurons are synchronised in the sense of having similar phases, but they are quiescent, not firing. The most likely phase of these quiescent neurons is given by the phase of z, as plotting in panel (b). The neurons

[1] The spatial domain was discretised with 100 equally-spaced points, and the trapezoidal rule used to evaluate the integral (16).

near the centre of the domain are firing, but at different rates, as shown by panel (c). We have repeated the simulations shown in Figs. 1 and 2 with $n = 3, 5, 10, \infty$ and found no qualitative differences between these cases, indicating that the precise value of n is not important.

The behaviour in the centre of the domain in Fig. 2 is worth commenting on. Consider a theta neuron with total input s: $d\theta/dt = 1 - \cos\theta + (1 + \cos\theta)s \equiv h(\theta, s)$. For $0 < s < 1$, h has a maximum at $\theta = \pi$ and minimum at 0, and thus the angular density (which is inversely proportional to velocity) has a maximum at 0 and minimum at π. The situation is reversed for $s > 1$, and the fact that the total input to neurons in the centre of the bump is greater than 1 is responsible for the two transitions of r through 0 and the corresponding jump of approximately π in ψ.

We can follow steady states of (19) as parameters are varied by spatially discretising and using standard algorithms [23]. An example is shown in Fig. 3 where we vary η_0, the average input to the network, ignoring coupling. We see that as η_0 is decreased, making it harder for neurons to fire, a stable bump is destroyed in a saddle-node bifurcation with an unstable bump. Profiles at two points on the curve are shown in panel (b).

We have presented only a "bump" state, to demonstrate the correspondence between a discrete network of theta neurons and the associated neural field model. However, a variety of other spatiotemporal patterns are of interest and have been studied elsewhere, including travelling fronts and bumps in one spatial dimension [3] and travelling waves [7], spiral waves [8] and target patterns [9] in two spatial dimensions. It would be of interest to investigate such patterns in a model like (19), knowing that there is a direct correspondence between this model and the corresponding network of theta neurons.

Several other generalisations of the results here can be mentioned. One involves including some kinetics in the synaptic coupling. As presented, the input to a neuron through the term I involves only the current state of neurons coupled to it. A simple modification would involve replacing kI_j in (1) by kb_j, where each b_j satisfies $db_j/dt = (I_j - b_j)/\tau$. Altering the time-constant τ would allow one to consider fast ($\tau \ll 1$) and slow ($\tau \gg 1$) synapses.

One could also include spike frequency adaptation, normally modelled by including a subtractive current proportional to the firing rate [3, 24], which is given by (22). More realistic neural field models include two populations, one excitatory and one inhibitory, with purely positive coupling between and within populations [10], and the network presented here is easily generalised to two such populations.

We finish by mentioning related work [25] in which these authors show that a particular form of the Winfree model of coupled oscillators, with coupling equivalent to the P_n that we use, can also be analysed exactly in the continuum limit using the Ott/Antonsen ansatz. The Winfree model includes a function referred to as the "phase response curve" which can be measured experimentally for an individual neuron [26], and the analysis of Pazó and Montbrió [25] relies on this being well-approximated by a sinusoidal function. While these authors did not consider spatially-extended networks, it would be straight forward to generalise their results to derive a spatially-extended model of a network of neurons, as we did here.

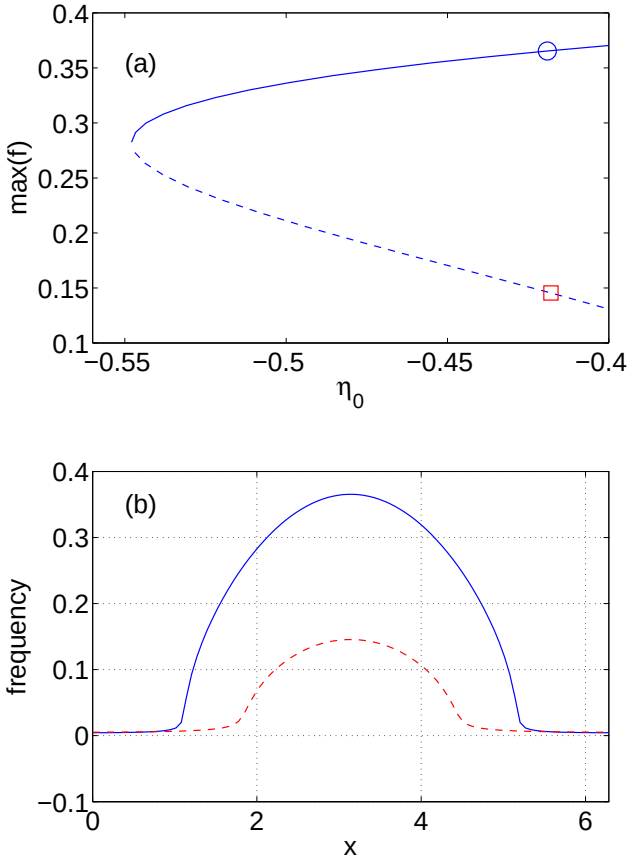

Figure 3: (Color online) (a): Maximum firing frequency in the network as a function of η_0. Solid: stable, dashed: unstable. (b): frequency profiles at the two points marked in (a) (solid blue curve, blue circle; dashed red curve, red square). Parameters: $L = 2\pi, k = 2, n = 2, \Delta = 0.02$.

[1] X.-J. Wang, Trends in Neurosciences **24**, 455 (2001).

[2] P. Jiruska, M. de Curtis, J. G. R. Jefferys, C. A. Schevon, S. J. Schiff, and K. Schindler, The Journal of Physiology **591**, 787 (2013).

[3] P. C. Bressloff, Journal of Physics A: Mathematical and Theoretical **45**, 033001 (2012).

[4] C. R. Laing and W. Troy, SIAM Journal on Applied Dynamical Systems **2**, 487 (2003).

[5] B. Ermentrout, Rep. Prog. Phys. **61**, 353 (1998).
[6] P. C. Bressloff and M. A. Webber, Journal of computational neuroscience **32**, 233 (2012).
[7] S. Coombes, N. A. Venkov, L. Shiau, I. Bojak, D. T. J. Liley, and C. R. Laing, Physical Review E **76**, 051901 (2007).
[8] C. R. Laing, SIAM Journal on Applied Dynamical Systems **4**, 588 (2005).
[9] Z. P. Kilpatrick and P. C. Bressloff, Journal of computational neuroscience **28**, 193 (2010).
[10] P. Blomquist, J. Wyller, and G. T. Einevoll, Physica D **206**, 180 (2005).
[11] K. Zhang, The journal of neuroscience **16**, 2112 (1996).
[12] B. Ermentrout, Neural computation **8**, 979 (1996).
[13] P. So, T. B. Luke, and E. Barreto, Physica D **267**, 16 (2014).
[14] T. B. Luke, E. Barreto, and P. So, Neural computation **25**, 3207 (2013).
[15] C. Laing and C. Chow, Neural Comput. **13**, 1473 (2001).
[16] A. Compte, N. Brunel, P. S. Goldman-Rakic, and X.-J. Wang, Cerebral Cortex **10**, 910 (2000).
[17] K. Wimmer, D. Q. Nykamp, C. Constantinidis, and A. Compte, Nature neuroscience **17**, 431 (2014).
[18] C. R. Laing, Physica D **238**, 1569 (2009).
[19] C. R. Laing, Physica D **240**, 1960 (2011).
[20] E. Ott and T. M. Antonsen, Chaos **19**, 023117 (2009).
[21] E. Ott and T. M. Antonsen, Chaos **18**, 037113 (2008).
[22] S. A. Marvel and S. H. Strogatz, Chaos **19**, 013132 (2009).
[23] E. Doedel, H. B. Keller, and J. P. Kernevez, International journal of bifurcation and chaos **1**, 493 (1991).
[24] J. Benda and A. V. Herz, Neural computation **15**, 2523 (2003).
[25] D. Pazó and E. Montbrió, Physical Review X **4**, 011009 (2014).
[26] N. W. Schultheiss, A. A. Prinz, and R. J. Butera, *Phase response curves in neuroscience: theory, experiment, and analysis* (Springer, 2011).